Methylene-to-Acetyl Conversion in Heterobinuclear Rh/Os Complexes: Models for Oxygenate Formation by Bimetallic Fischer−Tropsch Catalysts

Steven J. Trepanier, Robert McDonald,[‡] and Martin Cowie*[,§]

Department of Chemistry, University of Alberta Edmonton, Alberta, Canada T6G 2G2

Received April 16, 2003

Protonation of the methylene-bridged complex $[RhOs(CO)_3(\mu\text{-}CH_2)(\mu\text{-}CO)(dppm)_2][CF_3SO_3]$ with triflic acid at −80 °C yields the methyl complex $[RhOs(CO)_4(\mu\text{-}CH_3)(dppm)_2][CF_3SO_3]_2$ (**1**) in which the methyl group is primarily bound to Os while involved in an agostic interaction with Rh. Warming this species to −20 °C results in methyl migration to a terminal site on Rh, yielding $[RhOs(CH_3)(CO)_2(\mu\text{-}CO)_2(dppm)_2][CF_3SO_3]_2$ (**2**), and subsequent warming to ambient temperature results in migratory insertion to yield the acetyl-bridged $[RhOs(CF_3SO_3)(CO)_2(\mu\text{-}C(CH_3)O)(\mu\text{-}CO)(dppm)_2][CF_3SO_3]$ (**3**). Replacement of the coordinated triflate anion in **3** by CO and PMe_3 occurs at low temperature to give $[RhOs(L)(CO)_2(\mu\text{-}C(CH_3)O)(\mu\text{-}CO)(dppm)_2][CF_3SO_3]_2$ (L = CO (**4**), PMe_3 (**5a**)). Warming the PMe_3 adduct results in transformation of the acetyl group, which is C-bound to Rh in **5a**, to a group that is C-bound to Os in **5b**. One carbonyl in **3** is labile and is readily lost, yielding $[RhOs(CF_3SO_3)(CO)_2(\mu\text{-}C(CH_3)O)(dppm)_2][CF_3SO_3]$ (**6**). Attempts to obtain the above methyl or acetyl species by reaction of the hydride-bridged species $[RhOs(X)(CO)_3(\mu\text{-}H)(\mu\text{-}CO)(dppm)_2][X]$ (X = CF_3SO_3 (**7a**), BF_4 (**7b**)) with diazomethane were unsuccessful.

Introduction

As part of our continued interest in bimetallic compounds containing hydrocarbyl fragments having relevance to Fischer−Tropsch (FT) chemistry,[1] we have been pursuing chemistry resulting from the reactivity of methylene-bridged units in heterobinuclear Rh/Os,[2] Ir/Ru,[3] and Rh/Ru[4] complexes. Our primary interest has been in the involvement of methylene groups in carbon−carbon bond formation, seeking information on the steps in hydrocarbon formation. We are also interested in the mechanisms of oxygen incorporation into the hydrocarbons. Although the major products in the FT reaction are olefins and alkanes, oxygen-containing products such as alcohols, aldehydes, acids, and ketones are also obtained.[5] Historically, the formation of hydrocarbons for use as liquid fuels was the primary objective; however, emphasis has changed such that the generation of feedstocks for the chemical industry is now the primary objective.[1c,6] Among these feedstocks, oxygenates are of current interest and attempts are underway to optimize their production.[5,7] Some bimetallic catalysts involving late-metal combinations have been investigated for oxygenate formation; a rhodium−ruthenium-based catalyst has been developed that has a high selectivity for the production of ethylene glycol from syngas,[8] and several cobalt−ruthenium catalysts have been discovered that have a propensity for ethylene hydroformylation.[9] There is also considerable interest in the formation of alcohols such as methanol and ethanol, and catalysts involving Rh/Fe and Pd/Fe metal combinations have demonstrated higher activities and improved selectivities for methanol and ethanol production from syngas compared to their respective monometallic analogues.[10]

Although oxygenates are commonly produced in the FT reaction, little is known about the mechanisms involved in their formation. Based on analogies with the ubiquitous and well-studied migratory insertion of alkyl and carbonyl groups in transition metal complexes,[11] proposals have been put forward implicating this process in oxygenate formation in the FT reaction.[12] The so-formed acyl moiety could then react with other

* Corresponding author. E-mail: martin.cowie@ualberta.ca.
[‡] X-ray Crystallography Laboratory.
[§] Killam Annual Professor 2000/01.

(1) (a) Biloen, P.; Sachtler, W. M. H. *Adv. Catal.* **1981**, *30*, 165. (b) van der Laan, G. P.; Beenachers, A. A. C. M. *Catal. Rev.-Sci. Eng.* **1999**, *41*, 255. (c) Schulz, H. *Appl. Catal. A* **1999**, *186*, 3. (d) Maitlis, P. M.; Quyoum, R.; Long, H. C.; Turner, M. L. *Appl. Catal. A* **1999**, *186*, 363.

(2) Trepanier, S. J.; Sterenberg, B. T.; McDonald, R.; Cowie, M. *J. Am. Chem. Soc.* **1999**, *121*, 2613.

(3) Dell'Anna, M. M.; Trepanier, S. J.; McDonald, R.; Cowie, M. *Organometallics* **2001**, *20*, 88.

(4) Rowsell, B. D.; Trepanier, S. J.; Lam, R.; McDonald, R.; Cowie, M. *Organometallics* **2002**, *21*, 3228.

(5) (a) Vannice, M. A. *J. Catal.* **1975**, *37*, 449. (b) Verkerk, K. A. N.; Jaeger, B.; Finkeldai, C.-H.; Keim, W. *Appl. Catal. A* **1999**, *186*, 407. (c) Watson, P. R.; Samorjai, G. A. *J. Catal.* **1981**, *72*, 347.

(6) Overett, M. J.; Hill, R. O.; Moss, J. R. *Coord. Chem. Rev.* **2000**, *206−207*, 581.

(7) Ichikawa, M.; Fukuoka, A.; Xiao, F. *J. Catal.* **1992**, *138*, 206.

(8) Dombek, B. D. *Organometallics* **1985**, *4*, 1707.

(9) Ichikawa, M.; Xiao, F. *J. Catal.* **1994**, *147*, 578.

(10) (a) Ichikawa, M.; Fukuoka, A.; Hriljac, J. A.; Shriver, D. F. *Inorg. Chem.* **1987**, *26*, 3643. (b) Fukuoka, A.; Rao, L.-F.; Ichikawa, M. *Catal. Today* **1989**, *6*, 55. (c) Ichikawa, M.; Fukuoka, A.; Kimura, T. *Proceedings of the 9th International Congress on Catalysis*; Calgary, Chemical Institute of Canada: Ottawa, 1988; Vol. 2, p 258.

(11) Collman, J. P.; Hegedus, L. S.; Norton, J. R.; Finke, R. G. *Principles and Applications of Organotransition Metal Chemistry*; University Science Books: Mill Valley, CA, 1987; Chapter 6.

(12) (a) Pichler, H.; Schultz, H. *Chem. Ing. Technol.* **1970**, *12*, 1160. (b) Masters, C. *Adv. Organomet. Chem.* **1979**, *17*, 61. (c) Henrici-Olive, G.; Olive, S. *Angew. Chem., Int. Ed. Engl.* **1976**, *15*, 136.

10.1021/om030282m CCC: $25.00
Publication on Web 05/23/2003

surface fragments to produce the appropriate oxygenated compounds. Using bimetallic model complexes, it is possible to monitor potentially relevant reaction steps in the transformations and to study the mobilities of ligands and their migratory insertion tendencies on the bimetallic core. The carbonylation of methyl groups and subsequent reactivity has been studied to some extent in several dppm-bridged bimetallic systems (Rh/Rh,[13] Ru/Ru[14]) and an analogous dmpm-bridged diruthenium system (dmpm = $Me_2PCH_2PMe_2$).[15] We are interested in extending the investigation of migratory insertions to include combinations of different group 8/9 metals (Rh/Os, Ir/Ru), focusing on the roles of the different metals in the product formation. In this study we investigate the conversion of a bridging methylene group on a Rh/Os core into an acetyl group.

Experimental Section

General Comments. All solvents were dried (using appropriate drying agents), distilled before use, and stored under nitrogen. Reactions were performed under an argon atmosphere using standard Schlenk techniques. Rhodium(III) chloride trihydrate was purchased from Johnson Matthey Ltd., $Os_3(CO)_{12}$ was purchased from Strem, and PMe_3 (in THF), $HBF_4{\cdot}Me_2O$, and CF_3SO_3H were purchased from Aldrich. Carbon-13-enriched CO (99.4% enrichment) was purchased from Isotec Inc. The compounds $[RhOs(CO)_4(\mu\text{-}CH_2)(dppm)_2][X]$ (X = CF_3SO_3, BF_4) were prepared by the published procedure,[2] and $[RhOs(CO)_4(\mu\text{-}CD_2)(dppm)_2][CF_3SO_3]$ was prepared identically except using Diazald-*N*-methyl-d_3 to generate CD_2N_2.

NMR spectra were recorded on a Bruker AM-400 or Varian spectrometer operating at 400.1 MHz for ^1H, 161.9 MHz for ^{31}P, and 100.6 MHz for ^{13}C nuclei. Infrared spectra were obtained on a Nicolet Magna 750 FTIR spectrometer with a NIC-Plan IR microscope. The elemental analyses were performed by the microanalytical service within the department. Electron ionization mass spectra were run on a Micromass ZabSpec spectrometer. In all cases the distribution of isotope peaks for the appropriate parent ion matched very closely that calculated for the formulation given.

Spectroscopic data for all compounds are given in Table 1.

Preparation of Compounds. (a) $[RhOs(CO)_4(\mu\text{-}CH_3)(dppm)_2][CF_3SO_3]_2$ (1). Triflic acid (CF_3SO_3H) (0.7 μL, 0.0075 mmol) was added to a CD_2Cl_2 solution (0.5 mL) of $[RhOs(CO)_4(\mu\text{-}CH_2)(dppm)_2][CF_3SO_3]$ (10 mg, 0.0075 mmol) in an NMR tube at −78 °C. The solution changed from yellow to pale yellow. Compound **1** was characterized only spectroscopically since warming the solution to −20 °C resulted in conversion of **1** to compound **2**, and subsequent warming to ambient temperature resulted in further conversion to **3** as described below.

(b) $[RhOs(CH_2D)(CO)_4(dppm)_2][CF_3SO_3]_2$ (1-CH_2D). Deuterated triflic acid (CF_3SO_3D) (0.7 μL, 0.0075 mmol) was added to a CD_2Cl_2 solution (0.5 mL) of $[RhOs(CO)_4(\mu\text{-}CH_2)(dppm)_2][CF_3SO_3]$ (10 mg, 0.0075 mmol) in an NMR tube at −78 °C. NMR spectroscopy indicated a mixture of both **1** and **1**-CH_2D.

(c) $[RhOs(CHD_2)(CO)_4(dppm)_2][CF_3SO_3]_2$ (1-CHD_2). Triflic acid (CF_3SO_3H) (0.7 μL, 0.0075 mmol) was added to a CD_2Cl_2 solution (0.5 mL) of $[RhOs(CO)_4(\mu\text{-}CD_2)(dppm)_2][CF_3SO_3]$ (10 mg, 0.0075 mmol) in an NMR tube at −78 °C. NMR spectroscopy indicated a mixture of the three isotopomers **1**, **1**-CH_2D, and **1**-CHD_2.

(d) $[RhOs(CH_3)(CO)_4(dppm)_2][CF_3SO_3]_2$ (2). An NMR sample of **1** was prepared as outlined in part **(a)**. The sample was then warmed to −20 °C. Quantitative conversion of **1** to **2** occurred in approximately 1 h at this temperature. As was the case for **1** in part **(a)**, characterization of **2** was carried out spectroscopically since above −20 °C conversion to **3** occurred.

(e) $[RhOs(CF_3SO_3)(CO)_2(\mu\text{-}CO)(\mu\text{-}C(CH_3)O)(dppm)_2][CF_3SO_3]$ (3). The compound $[RhOs(CO)_4(\mu\text{-}CH_2)(dppm)_2][CF_3SO_3]$ (50 mg, 0.037 mmol) was dissolved in 5 mL of CH_2Cl_2, and CF_3SO_3H (3.3 μL, 0.037 mmol) was added, causing the solution to immediately change to pale yellow. The solution was stirred for 30 min, during which time the solution became yellow-orange. Ether (40 mL) was then added to precipitate an orange solid. This precipitate was washed with three 10 mL portions of diethyl ether and dried in vacuo (yield 82%). The solid also contained approximately 10% of an impurity identified as compound **6** (see below), which we failed to separate. Elemental analysis was not performed on this mixture of products; however the mass spectrum showed the expected parent ion without the triflate anion. MS: *m*/*z* 1339 ($M^+ - CF_3SO_3$). Compound **3**, with **6** as an accompanying impurity, was also obtained on warming a sample of **2** to ambient temperature.

(f) $[RhOs(CO)_4(\mu\text{-}C(CH_3)O)(dppm)_2][CF_3SO_3]_2$ (4). CO was passed through a solution of **3** in an NMR tube at −60 °C. The solution changed from yellow to pale yellow. Upon warming to room temperature, **4** converted to **3**. Characterization of **4** was by multinuclear NMR techniques at −60 °C.

(g) $[RhOs(CO)_3(PMe_3)(\mu\text{-}C(CH_3)O)(dppm)_2][CF_3SO_3]_2$ (5). A 1.0 M THF solution of PMe_3 (14 μL) was added to a CD_2Cl_2 solution (0.7 mL) of **3** (10 mg) in an NMR tube at −80 °C. Characterization of the first product **5a** was by multinuclear NMR techniques at −80 °C, since warming to ambient temperature resulted in quantitative transformation of this product into an isomer (**5b**). Spectroscopic data for the two species indicate that these isomers differ only in the coordination of the bridging acetyl group, which is C-bound to Rh in **5a** and to Os in **5b** (see Table 1 for spectroscopic data). Attempts to isolate **5b** as a solid led to decomposition to unidentified species.

(h) $[RhOs(CF_3SO_3)(CO)_2(\mu\text{-}C(CH_3)O)(dppm)_2][CF_3SO_3]$ (6). Compound **3** (30 mg, 0.02 mmol) was dissolved in 10 mL of CH_2Cl_2, and the solution was refluxed for 1 h under a slow argon purge. Ether (40 mL) was then added to precipitate an orange solid, which was recrystallized from CH_2Cl_2/ether and dried in vacuo (yield 90%). Anal. Calcd for $C_{56}H_{47}F_6O_9P_4S_2RhOs$: C, 46.06; H, 3.24. Found: C, 45.67; H, 3.27. MS: *m*/*z* 1311 ($M^+ - CF_3SO_3$).

(i) $[RhOs(CF_3SO_3)(CO)_4(\mu\text{-}H)(\mu\text{-}CO)(dppm)_2][CF_3SO_3]$ (7a). Triflic acid (7 μL, 0.076 mmol) was added to a CD_2Cl_2 solution (5 mL) of $[RhOs(CO)_4(dppm)_2][CF_3SO_3]$ (100 mg, 0.0076 mmol). The solution was stirred for 30 min and remained yellow. Ether (20 mL) was then added to precipitate a yellow solid, which was recrystallized from CH_2Cl_2/ether and dried in vacuo (yield 91%).

(j) $[RhOs(BF_4)(CO)_4(\mu\text{-}H)(\mu\text{-}CO)(dppm)_2][BF_4]$ (7b). A solution of HBF_4 in ether (11 μL, 0.079 mmol) was added to a CD_2Cl_2 solution (5 mL) of $[RhOs(CO)_4(dppm)_2][BF_4]$ (100 mg, 0.079 mmol). The solution was stirred for 30 min and remained yellow. Ether (20 mL) was then added to precipitate a yellow solid, which was recrystallized from CH_2Cl_2/ether and dried in vacuo (yield 86%). Anal. Calcd for $C_{54}H_{45}B_2F_8O_4P_4RhOs$: C, 48.09; H, 3.36. Found: C, 47.70; H, 3.26.

Attempted Reactions of 3, 5, and 6 with H_2. In each case 10 mg of the compound was dissolved in 0.7 mL of CD_2Cl_2 in a capped NMR tube, and dihydrogen was passed through the solution for long enough to displace the Ar atmosphere from above the solution. NMR monitoring of the solution of **3** showed only starting material. Even after storage of the sample under H_2 for 5 days, no reaction was observed. Addition of H_2 to a solution of **5a** caused the complete transformation to **5b** over

(13) Shafiq, F.; Kramarz, K. W.; Eisenberg, R. *Inorg. Chim. Acta* **1993**, *213*, 111.
(14) Gao, Y.; Jennings, M. C.; Puddephatt, R. J. *Organometallics* **2001**, *20*, 1882.
(15) Johnson, K. A.; Gladfelter, W. L. *Organometallics* **1990**, *9*, 2101.

Table 1. Spectroscopic Data for the Compounds

compound	IR (cm^{-1})[f]	NMR[a,b] $\delta(^{31}P\{^1H\})$[c]	$\delta(^1H)$[d,e]	$\delta(^{13}C\{^1H\})$[d]
$[RhOs(CH_3)(CO)_4(dppm)_2][CF_3SO_3]_2$ (**1**)		21.0 (m), −15.1 (m)	0.21(d, 3H, $^1J_{CH}$ = 125 Hz)[g], 3.72 (m, 2H), 3.98 (m,2H)	−32.2 (s, br), 20.2 (m, 2C),[h]170.3 (br), 171.2 (br), 201.9 (dt, $^2J_{PC}$ = 8 Hz, $^1J_{RhC}$ = 23 Hz), 185.6 (dt, $^2J_{PC}$ = 14 Hz, $^1J_{RhC}$ = 82 Hz)
$[RhOs(CH_3)(CO)_4(dppm)_2][CF_3SO_3]_2$ (**2**)		28.9 (m), −10.7 (m)	1.65 (ddt, 3H, $^1J_{CH}$ = 139 Hz, $^3J_{PH}$ = 7 Hz, $^2J_{RhH}$ = 9 Hz)[g]	43.1 (d, $^1J_{Rh-C}$ = 25 Hz), 167.2 (m, 2C, $^2J_{PC}$ = 7 Hz), 210.9 (dm, 2C, $^1J_{RhC}$ = 25 Hz)
$[RhOs(CF_3SO_3)(CO)_3(\mu\text{-}CH_3CO)(dppm)_2][CF_3SO_3]$ (**3**)	2070 (s),1989 (s), 1715 (s)	5.5 (dm, $^1J_{RhP}$ = 150 Hz), −5.0 (m)	2.08 (s, 3H), 3.22 (m, 4H)	22.5 (m, 2C),[h]46.6 (s, br), 313.3 (dm, $^1J_{RhC}$ = 42 Hz), 239.9 (m), 174.7 (t, $^2J_{PC}$ = 6 Hz), 174.2 (m, br)
$[RhOs(CO)_4(\mu\text{-}CH_3CO)(dppm)_2][CF_3SO_3]_2$ (**4**)		13.3 (dm, $^1J_{RhP}$ = 128 Hz), −4.5 (m)	1.81 (s, 3H), 3.44 (m, 2H), 3.86 (m, 2H)	321.8 (dm, $^1J_{RhC}$ = 30 Hz), 223.9 (m), 187.6 (dm, $^1J_{RhC}$ = 47 Hz), 172.3 (s, br), 171.4 (s, br)
$[RhOs(CO)_3(PMe_3)(\mu\text{-}CH_3CO)(dppm)_2][CF_3SO_3]_2$ (**5a**)	2070 (s), 2008 (s), 1727 (m)	14.5 (dm, $^1J_{RhP}$ = 137 Hz), −3.9 (m), −38.3 (ddt, $^1J_{RhP}$ = 101 Hz)	0.91 (d, 9H; $^2J_{PH}$ = 8 Hz), 1.82 (s, 3H), 3.07 (m, 2H), 3.48 (m, 2H)	325.8 (ddt, $^1J_{RhC}$ = 30 Hz, $^2J_{P(PMe_3)C}$ = 82 Hz; $^2J_{PC}$ = 9 Hz), 237.0 (m), 174.8 (s, br), 171.2 (m)
$[RhOs(CO)_3(PMe_3)(\mu\text{-}CH_3CO)(dppm)_2][CF_3SO_3]_2$ (**5b**)	2067 (s), 1991(s), 1735 (m)	22.8 (dm, $^1J_{RhP}$ = 125 Hz), −8.8 (m), −9.5(dt, $^1J_{RhP}$ = 100 Hz; $^2J_{PP}$ = 32 Hz)	0.98 (d, 9H; $^2J_{PH}$ = 10 Hz), 2.04 (s, 3H), 3.99 (m, 2H), 3.74 (m, 2H)	293.4 (m), 218.1 (m), 183.0 (m), 172.5 (m)
$[RhOs(CF_3SO_3)(CO)_2(\mu\text{-}CH_3CO)(dppm)_2][CF_3SO_3]$ (**6**)	2033 (s), 1974 (s), 1436 (m)	16.6 (m), −4.7 (m)	2.03 (s, 3H), 2.60 (m, 2H), 3.92 (m, 2H)	274.2 (dt, $^1J_{RhC}$ = 31 Hz, $^2J_{PC}$ = 8 Hz), 181.6 (t, $^2J_{PC}$ = 6 Hz), 163.2 (dt, $^2J_{PC}$ = 7 Hz; $^2J_{RhC}$ = 7 Hz)
$[RhOs(CF_3SO_3)(CO)_4(\mu\text{-}H)(dppm)_2][CF_3SO_3]$ (**7a**)	2092 (m), 2045 (s), 2010 (s), 1870 (m)	27.2 (m), −7.3 (m)	−10.46 (dtt, 1H; $^1J_{RhH}$ = 21 Hz, $^2J_{P(Rh)H}$ = 9 Hz, $^2J_{P(Os)H}$ = 8 Hz), 4.92 (m, 4H), 4.31(m, 2H)	200.0 (br); 171.8 (br), 169.4 (s), 181.8 (dt, $^1J_{RhC}$ = 79 Hz; $^2J_{PC}$ = 15 Hz)
$[RhOs(BF_4)(CO)_4(\mu\text{-}H)(dppm)_2][BF_4]$ (**7b**)[i]	2096 (m), 2052 (s), 1983 (s), 1871 (m)	27.5 (m), −6.7 (m)	4.52 (m, 2H), 4.25 (m, 2H), −11.00 (dtt, 1H, $^1J_{RhH}$ = 22 Hz, $^2J_{P(Os)H}$ = 11 Hz, $^2J_{P(Rh)H}$ = 8 Hz)	200.7 (br); 171.9 (br), 170.6 (s), 182.7 (dt, $^1J_{RhC}$ = 79 Hz; $^2J_{PC}$ = 15 Hz)

[a] NMR abbreviations: s = singlet, d = doublet, t = triplet, m = multiplet, dt = doublet of triplets, dm = doublet of multiplets, ddt = doublet of doublets of triplets, br = broad. [b] NMR data at 298 K in CD_2Cl_2 unless otherwise stated. [c] $^{31}P\{^1H\}$ NMR chemical shifts are referenced vs external 95% H_3PO_4. [d] ^1H and ^{13}C chemical shifts are referenced vs external TMS. [e] Chemical shifts for the phenyl hydrogens are not given. [f] All samples run as solids. IR abbreviations (ν(CO) unless otherwise stated): s = strong, m = medium. [g] For $^{13}CH_3$-enriched product. [h] ^{13}C resonances for methylene carbons of the dppm ligands. [i] Although this compound was previously reported (ref 16), it had not been identified as containing coordinated BF_4^- anion or fully characterized.

a 4 h period. Although no further reaction was noted within this time, complete conversion to $[RhOs(\mu\text{-}H)_2(CO)_3(dppm)_2][CF_3SO_3]$,[16] CH_4, CO, and $[HPMe_3][CF_3SO_3]$ was observed after 36 h, as detected by ^1H, ^{31}P, and ^{13}C NMR spectroscopy. No immediate reaction was observed between compound **6** and H_2. However, after several days a complex mixture of unidentified products was observed by NMR.

X-ray Data Collection. Pale yellow crystals of $[RhOs(CO)_2(O_3SCF_3)(\mu\text{-}CO)(\mu\text{-}C(CH_3)O)(dppm)_2][BF_4]\cdot 2.5CH_2Cl_2$ (**3**) were obtained via slow evaporation of a dichloromethane solution of the complex. Data were collected on a Bruker PLATFORM/SMART 1000 CCD diffractometer[17] using Mo Kα radiation at −80 °C. Unit cell parameters were obtained from a least-squares refinement of the setting angles of 7281 reflections from the data collection. The space group was determined to be $P2_1/n$ (an alternate setting of $P2_1/c$ [No.14]). The data were corrected for absorption through use of the SADABS procedure. See Table 2 for a summary of crystal data and X-ray data collection information.

Orange crystals of $[RhOs(CO)_2(O_3SCF_3)(\mu\text{-}C(CH_3)O)(dppm)_2][CF_3SO_3]\cdot 2CH_2Cl_2$ (**6**) were obtained via slow diffusion of diethyl ether into a dichloromethane solution of the compound. Data were collected and corrected for absorption as for **3** above (see Table 2). Unit cell parameters were obtained from a least-squares refinement of the setting angles of 6151 reflections from the data collection, and the space group was determined to be $P2_12_12_1$ (No. 19).

Yellow crystals of $[RhOs(O_3SCF_3)(CO)_3(\mu\text{-}H)(\mu\text{-}CO)(dppm)_2][CF_3SO_3]\cdot 2H_2O$ (**7a**) were obtained as for **6**. Data were collected and corrected as outlined in Table 2. Unit cell parameters were obtained from a least-squares refinement of the setting angles of 4220 reflections from the data collection, and the space group was determined to be $Pca2_1$ (No. 29).

Structure Solution and Refinement. The structure of **3** was solved using automated Patterson location of the heavy metal atoms and structure expansion via the DIRDIF-96 program system.[18] Refinement was completed using the program SHELXL-93.[19] Hydrogen atoms were assigned positions

(16) Hilts, R. W.; Franchuk, R. A.; Cowie, M. *Organometallics* **1991**, *10*, 304.

(17) Programs for diffractometer operation, data collection, data reduction, and absorption correction were those supplied by Bruker.

Table 2. Crystallographic Experimental Details for Compounds 3, 6, and 7a

	3	**6**	**7a**
formula	$C_{58.5}H_{52}BCl_5F_7O_7OsP_4RhS$	$C_{58}H_{51}Cl_4F_6O_9OsP_4RhS_2$	$C_{56}H_{49}F_6O_{12}OsP_4RhS_2$
fw	1637.11	1628.90	1509.06
cryst dimens (mm)	0.72 × 0.17 × 0.03	0.30 × 0.19 × 0.07	0.41 × 0.08 × 0.06
cryst syst	monoclinic	orthorhombic	orthorhombic
space group	$P2_1/n$ (an alternate setting of $P2_1/c$ [No. 14])	$P2_12_12_1$ (No. 19)	$Pca2_1$ (No. 29)
unit cell params			
a (Å)	10.2572 (10)[a]	14.5915 (7)[b]	24.229(2)[c]
b (Å)	24.675 (2)	17.0016 (8)	22.8565(10)
c (Å)	25.890 (2)	24.6970 (12)	23.376(2)
β (deg)	95.4565 (19)	90	90
V (Å^3)	6522.9 (11)	6126.8 (5)	6715.3(10)
Z	4	4	4
ρ_{calcd} (g cm^{-3})	1.667	1.766	1.493
μ (mm^{-1})	2.603	2.762	2.363
diffractometer	Bruker PLATFORM/SMART 1000 CCD		
radiation (λ [Å])	graphite-monochromated Mo Kα (0.71073)		
temperature (°C)	−80	−80	−80
scan type	ω scans (0.2°) (20 s exposures)	ω scans (0.2°) (20 s exposures)	ω scans (0.2°) (30 s exposures)
data collection 2θ limit (deg)	52.84	52.82	52.82
total data collected	34 036 ($-12 \le h \le 11$, $-30 \le k \le 30$, $-32 \le l \le 28$)	28 744 ($-18 \le h \le 11$, $-20 \le k \le 21$, $-30 \le l \le 30$)	30 173 ($-29 \le h \le 30$, $-14 \le k \le 12$, $-29 \le l \le 29$)
no. of ind reflns	13 179 (R_{int} = 0.0588)	12 533 (R_{int} = 0.0378)	13 495 (R_{int} = 0.0500)
no. of obsd reflns	10 092 [$F_o^2 \ge 2\sigma(F_o^2)$]	11 389 [$F_o^2 \ge 2\sigma(F_o^2)$]	10 069 [$F_o^2 \ge 2\sigma(F_o^2)$]
structure solution method	Patterson search/structure expansion (*DIRDIF-96*)		
refinement method	full-matrix least-squares on F^2 (*SHELXL-93*[d])		
abs corr method	multiscan (*SADABS*)		
range of transmn factors	0.9260−0.2558	0.8302−0.4912	0.8712−0.4442
no. of data/restraints/params	13 179 [$F_o^2 \ge -3\sigma(F_o^2)$]/7[e]/763	12 533 [$F_o^2 \ge -3\sigma(F_o^2)$]/0/768	13 495 [$F_o^2 \ge -3\sigma(F_o^2)$]/3[f]/658
Flack absolute structure param[g]		0.485 (4)	0.016(8)
goodness-of-fit (S)[h]	1.049 [$F_o^2 \ge -3\sigma(F_o^2)$]	1.041 [$F_o^2 \ge -3\sigma(F_o^2)$]	1.068 [$F_o^2 \ge -3\sigma(F_o^2)$]
final R indices[i]			
R_1 [$F_o^2 \ge 2\sigma(F_o^2)$]	0.0544	0.0339	0.0563
wR_2 [$F_o^2 \ge -3\sigma(F_o^2)$]	0.1475	0.0766	0.1520
largest difference peak and hole (e Å^{-3})	1.867 and −1.659	1.257 and −0.593	1.713 and −0.942

[a] Obtained from least-squares refinement of 7281 centered reflections. [b] Obtained from least-squares refinement of 6151 centered reflections. [c] Obtained from least-squares refinement of 4220 centered reflections. [d] Refinement on F_o^2 for all reflections (all of these having $F_o^2 \ge -3\sigma(F_o^2)$). Weighted R-factors wR_2 and all goodnesses of fit S are based on F_o^2; conventional R-factors R_1 are based on F_o, with F_o set to zero for negative F_o^2. The observed criterion of $F_o^2 > 2\sigma(F_o^2)$ is used only for calculating R_1 and is not relevant to the choice of reflections for refinement. R-factors based on F_o^2 are statistically about twice as large as those based on F_o, and R-factors based on ALL data will be even larger. [e] The S−C (1.80 Å) and F−C (1.35 Å) distances within the minority (1/3) conformer for the coordinated triflate group were assigned fixed idealized values, as were interatomic distances within the half-occupancy solvent dichloromethane molecule (d(Cl(5S)−C(3S)) = d(Cl(6S)−C(3S)) = 1.80 Å; d(Cl(5S)···Cl(6S)) = 2.95 Å). [f] The bridging hydrido ligand (H(1)) was refined with an idealized geometry by fixing the Os−H and Rh−H distances at 1.85 Å and by constraining the Os, Rh, C(3), and H(1) atoms to planarity. [g] Flack, H. D. *Acta Crystallogr.* **1983**, *A39*, 876. The Flack parameter will refine to a value near zero if the structure has the correct configuration and near one for the inverted configuration. The value observed for compound **6** is indicative of racemic twinning and was accommodated during refinement using the SHELXL-93 TWIN instruction (see ref 19). [h] $S = [\sum w(F_o^2 - F_c^2)^2/(n-p)]^{1/2}$ (n = number of data; p = number of parameters varied; $w = [\sigma^2(F_o^2) + (a_0P)^2 + a_1P]^{-1}$ where $P = [\mathrm{Max}(F_o^2, 0) + 2F_c^2]/3$), and the values of a_0 and a_1 are adjusted by the refinement program; for **3**, a_0 = 0.0738, a_1 = 21.7034; for **6**, a_0 = 0.0402, a_1 = 0; for **7a**, a_0 = 0.0775, a_1 = 0). [i] $R_1 = \sum||F_o| - |F_c||/\sum|F_o|$; $wR_2 = [\sum w(F_o^2 - F_c^2)^2/\sum w(F_o^4)]^{1/2}$.

based on the geometries of their attached carbon atoms and were given thermal parameters 20% greater than those of the attached carbons. The coordinated triflate group was disordered over two orientations in a 2:1 ratio, having a common site for the oxygen coordinated to Rh. An idealized geometry was imposed upon the minority (1/3) conformer for the coordinated triflate group by assigning fixed idealized values to the S−C (1.80 Å) and F−C (1.35 Å) distances; interatomic distances within the half-occupancy solvent dichloromethane molecule were also assigned idealized values (d(Cl(5S)−C(3S)) = d(Cl(6S)−C(3S)) = 1.80 Å; d(Cl(5S)···Cl(6S)) = 2.95 Å). The final model for **3** refined to values of $R_1(F)$ = 0.0544 (for 10 092 data with $F_o^2 \ge 2\sigma(F_o^2)$) and $wR_2(F^2)$ = 0.1475 (for all 13 179 independent data).

The structures of **6** and **7a** were also solved using the DIRDIF-96 program system in the same manner as for **3** above. Refinement was completed using the program SHELXL-93, during which the hydrogen atoms were treated as for **3**. The final model for **6** refined to values of $R_1(F)$ = 0.0339 (for 11 389 data with $F_o^2 \ge 2\sigma(F_o^2)$) and $wR_2(F^2)$ = 0.0766 (for all 12 533 independent data).

For compound **7a** two water molecules were located in the unit cell. The final model converged to R_1 = 0.0503 for 10 069 reflections with $F_o^2 \ge 2\sigma(F_o^2)$ and $wR_2(F^2)$ = 0.1520 for all 13 495 independent data.

Results and Compound Characterization

Protonation of the methylene-bridged compound [Rh-Os(CO)$_3$(μ-CO)(μ-CH$_2$)(dppm)$_2$][CF$_3$SO$_3$], using triflic

(18) Beurskens, P. T.; Beurskens, G.; Bosman, W. P.; deGelder, R.; Garcia Granda, S.; Gould, R. O.; Israel, R.; Smits, J. M. M. *The DIRDIF-96 program system*; Crystallography Laboratory, University of Nijmegen: The Netherlands, 1996.

(19) Sheldrick, G. M. *SHELXL-93*. Program for crystal structure determination; University of Göttingen: Germany, 1993.

Scheme 1

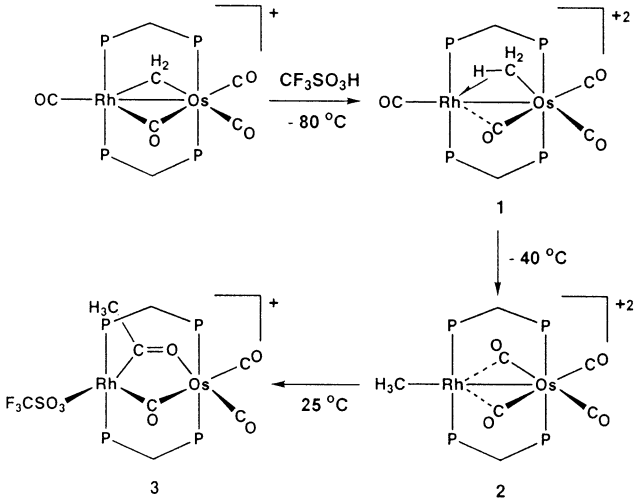

acid (CF_3SO_3H), at −80 °C yields a dicationic methyl compound, $[RhOs(CO)_4(CH_3)(dppm)_2][CF_3SO_3]_2$ (**1**) (Scheme 1). No evidence of a methylene-bridged hydride species resulting from protonation at either metal was observed. $^1H/^{31}P$ NMR correlation spectroscopy shows strong coupling between the osmium-bound phosphines and the methyl protons and a much weaker coupling between the rhodium-bound phosphines and the methyl group. This suggests that the methyl group is primarily bound to osmium but that there is also a weak interaction between the methyl protons and rhodium. The observed ^1H resonance is broad at −80 °C, sharpening somewhat, but not resolving, at −40 °C. The spectra of **1** could not be obtained at higher temperatures since it transforms to a new compound (**2**). At lower temperatures (−100 °C) the signal breadth increases.

The coupling of the methyl protons to the phosphines on both metals suggests that this group may be bridging. To investigate this further, the isotopomers of **1** incorporating CH_3, CH_2D, and CHD_2 groups were prepared. The CH_2D isotopomer (**1**-CH_2D) was obtained by reaction of $[RhOs(CO)_3(\mu\text{-}CO)(\mu\text{-}CH_2)(dppm)_2][CF_3SO_3]$ with CF_3SO_3D, whereas **1**-CHD_2, (as well as amounts of the other isotopomers) was obtained by protonation of $[RhOs(CO)_3(\mu\text{-}CO)(\mu\text{-}CD_2)(dppm)_2][CF_3SO_3]$. At −40 °C the CH_3 methyl resonance of **1** is observed at δ 0.25 in the ^1H NMR spectrum, whereas the signal for **1**-CH_2D appears at δ 0.07 and that for **1**-CHD_2 is further upfield shifted to δ −0.15 (see Figure 1).

The shift of the ^1H NMR resonance of a methyl group to higher fields as the deuteration is increased is characteristic of an agostic interaction. Due to the lower zero-point energy of a C−D bond relative to C−H, an agostic interaction involving a C−H bond (**A** in Chart 1) is favored over that involving a C−D bond (**B**). Thus, as the deuteration is increased, the remaining proton(s) in the isotopomers of the methyl group will spend an increased amount of time bound to the rhodium center (**A**), leading to upfield chemical shifts for the protons in the ^1H NMR spectrum. A similar agostic interaction of a methyl group has recently been reported in a dppm-bridged diruthenium complex.[14] This NMR technique, called isotopic perturbation of resonance

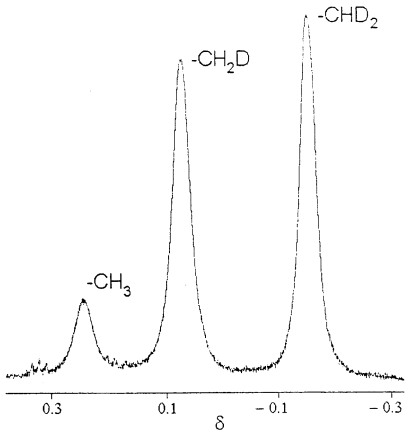

Figure 1. ^1H NMR spectrum in the methyl region for the three methyl isotopomers **1**, **1**-CH_2D, and **1**-CHD_2.

Chart 1

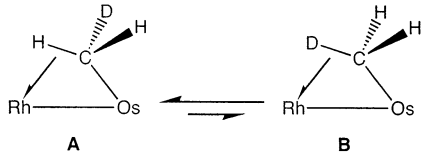

Chart 2

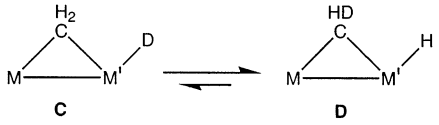

(IPR), was first described by Saunders[20] in studies of carbocations, but was later developed by Shapley[21] and others[22,23] to investigate the agostic bonding of bridging methyl groups in transition metal complexes.

The IPR effect observed here could also be a consequence of a rapidly exchanging bridging-methylene/hydride complex (Chart 2) as recently reported in a dppm-bridged diiridium compound.[24] In a methylene-bridged hydride structure such as **C** or **D** zero-point energy effects favor retention of a C−D bond (**D**) over a C−H bond (**C**), resulting in a similar upfield ^1H NMR signal as deuteration increases.[25] In the aforementioned diiridium complex, the sharp ^1H resonance observed at ambient temperature collapsed into the baseline at ca. −60 °C, and by −100 °C two broad resonances (at δ 4.2 and −14.6) for the methylene and hydride signals, respectively, had started to emerge.[24] For compound **1** the low-temperature limiting structure has not been observed at −100 °C, as the signal remains broad at this temperature, indicating a lower activation energy

(20) Saunders, M.; Jaffe, M. H.; Vogel, P. *J. Am. Chem. Soc.* **1971**, *93*, 2558.
(21) Calvert, R. B.; Shapley, J. R. *J. Am. Chem. Soc.* **1978**, *100*, 7726.
(22) Dawkins, G. M.; Green, M.; Orpen, A. G.; Stone, F. G. A. *J. Chem. Soc., Chem. Commun.* **1982**, 41.
(23) (a) Casey, C. P.; Fagan, P. J.; Miles, W. H. *J. Am. Chem. Soc.* **1982**, *104*, 1134. (b) Green, M. L. H.; Hughes, A. K.; Popham, N. A.; Stephens, A. H. H.; Wong, L.-L. *J. Chem. Soc., Dalton Trans.* **1992**, 3077.
(24) Torkelson, J. R.; Antwi-Nsiah, F. H.; McDonald, R.; Cowie, M.; Pruis, J. G.; Talkanen, K. J.; DeKock, R. L. *J. Am. Chem. Soc.* **1999**, *121*, 3666.
(25) (a) Brookhart, M.; Green, M. L. H.; Wong, L.-L. *Prog. Inorg. Chem.* **1988**, *36*, 1. (b) Tolman, C. A.; Faller, J. W. In *Homogeneous Catalysis with Metal Phosphine Complexes*; Pignolet, L. H., Ed.; Plenum Press: New York, 1983; pp 30−34.

than observed for the C−H activation step in the "Ir_2" complex, suggesting to us that equilibration of an agostic structure by methyl rotation about the Os−CH_3 bond is occurring, as shown by the process in Chart 1.

In principle, further evidence for agostic bonding involving a bridging methyl group is the reduced $^1J_{CH}$ value for this group. However, the observed average $^1J_{CH}$ value of 125 Hz in a $^{13}CH_3$-enriched sample of compound **1** lies in the normal range for terminally bound methyl groups, which can lie between 120 and 145 Hz for late-metal complexes.[26] Nevertheless, the observed value is close to the 121 Hz observed in $[Os_3(CO)_{10}(\mu\text{-H})(\mu\text{-CH}_3)]$[21] and $[Cp_2Fe_2(CO)_2(\mu\text{-CH}_3)(\mu\text{-CO})]$,[23a] which have been shown to have bridged agostic methyl groups, and is significantly less than the 139 Hz observed in compound **2** (vide infra), in which the methyl group adopts a conventional η^1 binding mode. In a methylene-bridged hydride complex, coupling between the methylene carbon and the hydride ligand should be close to 0 Hz, giving rise to an average coupling of ca. 93 Hz (assuming $^1J_{C-H} = 140$ Hz for a methylene group),[23,24,25a] as observed in the Ir_2 compound. Clearly, the observed $^1J_{C-H}$ value for **1** is inconsistent with a methylene−hydride exchange process and is instead consistent with an asymmetrically bridged methyl group.

In the $^{13}C\{^1H\}$ NMR spectrum at −60 °C, the methyl resonance appears as a broad singlet at δ −32.2; no coupling to the ^{31}P or ^{103}Rh nuclei is evident. The high-field chemical shift of this carbon is also supportive of an agostic methyl group rather than a methylene-hydride complex and can be contrasted to the ^{13}C resonance at δ +36.1 observed for the methylene carbon in the diiridium species.[24] Furthermore, the lack of coupling between this carbon and rhodium is clearly inconsistent with a bridging methylene group and again suggests a weak agostic interaction between a methyl group and rhodium. In the carbonyl region, two broad signals at δ 170.3 and 171.2 are assigned to osmium-bound carbonyls since they show no rhodium coupling, whereas a doublet of triplets at δ 185.6 corresponds to a rhodium-bound carbonyl ($^1J_{Rh-C} = 82$ Hz, $^2J_{P(Rh)-C} = 14$ Hz). A fourth signal, a doublet of triplets at δ 201.9, is assigned to a semibridging carbonyl on the basis of the rhodium coupling ($^1J_{Rh-C}$) of 23 Hz as well as a lower coupling constant with the osmium-bound phosphorus nuclei ($^2J_{P(Os)-C} = 8$ Hz) compared to the terminally bound carbonyls. The downfield chemical shift of this carbonyl is also characteristic of a semibridging carbonyl.

Upon warming a solution of **1** to −20 °C, a new compound, $[RhOs(CH_3)(CO)_4(dppm)_2][CF_3SO_3]_2$ (**2**), forms. This product is an isomer of **1**, which now contains a rhodium-bound methyl group (see Scheme 1). In the ^1H NMR spectrum this methyl group appears at δ 1.65 as a doublet of triplets due to coupling to rhodium ($^2J_{Rh-H} = 9$ Hz) and the rhodium-bound phosphines ($^3J_{P-H} = 7$ Hz). As noted earlier, the C−H coupling of 139 Hz, when the methyl group is ^{13}C-enriched, is consistent with a terminally bound methyl ligand. The dppm methylene protons appear as a single multiplet indicating front/back symmetry in the molecule, in contrast to the two dppm resonances observed in **1**, where the environment on one side of the $RhOsP_4$ plane differs from that on the other. The $^{13}C\{^1H\}$ NMR spectrum of **2** contains two resonances in the carbonyl region; the resonance at δ 167.2 represents two equivalent osmium-bound carbonyls, and the signal at δ 210.9 is assigned to two equivalent osmium-bound carbonyls having a semibridging interaction with the rhodium center ($^1J_{Rh-C} = 25$ Hz). The chemical shift of the methyl carbon appears at δ 43.1, considerably downfield with respect to its precursor **1**, in which the methyl group was bound to osmium, and the coupling of this methyl carbon to Rh ($^1J_{Rh-C} = 25$ Hz) unambiguously establishes the connectivity for **2**. A downfield shift for the rhodium-bound methyl group compared to that bound to Os was also seen in the dimethyl compound $[RhOs(CH_3)_2(CO)_3(dppm)_2][CF_3SO_3]$, in which the osmium-bound methyl group appears at δ −18.1, while that bound to rhodium appears at δ 22.8.[27]

Upon warming to ambient temperature, compound **2** transforms into yet another compound, $[RhOs(CF_3SO_3)(CO)_2(\mu\text{-CO})(\mu\text{-C}(CH_3)O)(dppm)_2][CF_3SO_3]$ (**3**), as can be seen in the ^{31}P NMR spectrum, where new resonances at δ 5.5 and −5.0 appear; the low-field signal represents the rhodium-bound phosphorus nuclei ($^1J_{Rh-P} = 150$ Hz). The pattern of this signal is characteristic of a "$RhOs(dppm)_2$" complex in which there is no metal−metal bond. In similar, bis dppm-bridged compounds containing metal−metal bonds, the intraligand P−P coupling is comparable to the Rh−P coupling, resulting in an observed $^{31}P\{^1H\}$ signal for the rhodium-bound phosphines that is best described as a multiplet.[27,28] In non-metal−metal bonded species the absence of a metal−metal bond results in a decrease in the P−P couplings, resulting in a signal that can be described as a doublet of pseudo-triplets. In the ^1H NMR spectrum the methyl group appears as a sharp singlet at δ 2.08, indicating no coupling to either ^{31}P or ^{103}Rh nuclei. When a ^{13}CO-enriched sample was examined, the methyl protons appear as a doublet signal with coupling to a carbonyl carbon ($^2J_{C-H} = 4$ Hz). This suggests the assignment $[RhOs(CF_3SO_3)(CO)_2(\mu\text{-CO})(\mu\text{-C}(CH_3)O)(dppm)_2][CF_3SO_3]$ for **3** shown in Scheme 1, in which an acetyl group has formed by migratory insertion. Although the dppm-methylene protons appear as a single multiplet, suggesting a front/back symmetry to the molecule, the subsequent structural determination (vide infra) clearly indicates that the proposed structure is correct, in which the acyl group bridges the metals, indicating an accidental equivalence of the two inequivalent dppm-methylene protons.

Support for the acyl formulation comes from the ^{13}C NMR spectrum, in which the acyl carbon resonates at δ 313.3, showing a strong coupling to Rh ($^1J_{Rh-C} = 42$ Hz). The significant downfield shift of this carbon is characteristic of a bridging acyl group and suggests some degree of carbene character,[15,29] and can be contrasted to terminally bound acyl groups that typi-

(26) See for example: (a) Kulzick, M. A.; Price, R. T.; Andersen, R. A.; Muetterties, E. L. *J. Organomet. Chem.* **1987**, *333*, 105. (b) Siedle, A. R.; Newmark, R. A.; Pignolet, L. H. *Organometallics* **1984**, *3*, 855. (c) Haynes, A.; Mann, B. E.; Morris, G. E.; Maitlis, P. M. *J. Am. Chem. Soc.* **1993**, *115*, 4093.

(27) Sterenberg, B. T., Ph.D. Thesis, University of Alberta, 1997, Chapter 2.

(28) Antonelli, D. M., Ph.D. Thesis, University of Alberta, 1991.

(29) Jeffrey, J. C.; Orpen, A. G.; Stone, F. G. A.; Went, M. J. *J. Chem. Soc., Dalton Trans.* **1986**, 173.

Chart 3

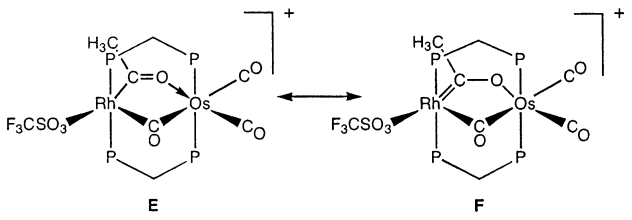

cally appear in the δ 230−260 range in the ^{13}C NMR spectrum.[13−15,29] Similar downfield shifts have been observed in other binuclear dppm- or dmpm-bridged systems (Rh−Rh,[13] Ru−Ru[14,15]) containing bridging acetyl groups, and these complexes have also been assigned carbene character. This bridging mode allows for two resonance structures as depicted in Chart 3, the latter of which (**F**) contributes to the observed low-field ^{13}C shift.

Also, in the $^{13}C\{^1H\}$ NMR spectrum the bridging carbonyl resonance appears as a low-field multiplet at δ 239.9; the coupling to Rh could not be resolved owing to coupling to the phosphines and to the other carbonyls. The terminal carbonyls appear at δ 174.7 and 174.2 and are established as being bound to osmium on the basis of the absence of Rh coupling. The methyl carbon of the acyl group, at δ 46.6, is slightly broad, possibly indicating a small unresolved coupling to rhodium. The IR spectrum is also consistent with this formulation, showing a bridging carbonyl stretch at a characteristic low frequency (1715 cm^{-1}). Unfortunately, no stretch corresponding to the acyl carbonyl was observed, even using comparisons with the spectrum for the ^{13}CO-labeled sample.

The above structural assignment for **3** has been confirmed by an X-ray structure determination, which clearly shows the bridging acyl/bridging carbonyl arrangement, in which the acyl group is carbon-bound to rhodium and oxygen-bound to osmium (see Figure 2). Bond lengths and angles are summarized in Table 3. Both dppm ligands have the normal "trans-bridging" arrangement typical of "A-frame" complexes. About Os, the geometry is octahedral, having mutually trans phosphine ligands and the mutually cis bridging acyl and carbonyl groups opposite the two terminal carbonyls. At rhodium, the geometry is a distorted tetragonal pyramid in which two sites are occupied by the trans phosphines (P(2)−Rh−P(4) = 171.16(7)°) and the other three by the acyl carbon, the bridging carbonyl, and a triflate anion (opposite the acyl group). The coordination site opposite the apical bridging carbonyl is vacant. The geometry at the bridging acyl group is consistent with sp^2 hybridization of the acyl carbon with angles at C(4) of approximately 120°. Both the short Rh−C(4) (1.907(7) Å) and the long C(4)−O(4) (1.258(8) Å) distances are consistent with a high degree of carbene character;[30] the Rh−C(4) distance is substantially shorter than typical acetyl groups and is even shorter than that reported for a carbene-like acyl group in $[Rh_2(CO)_2(\mu\text{-}C(CH_3)O)(dppm)_2][CF_3SO_3]$ (2.05(2) Å).[13] Certainly the Rh−acyl distance in **3** is comparable to the Os−CO distances for which significant π back-bonding is assumed (cf. Os−C(1), Os−C(2) = 1.957(8), 1.873(7) Å). Similarly, the C(4)−O(4) distance is substantially longer than observed in normal η^1-acetyl groups and is comparable to that reported by Eisenberg (1.28(2) Å).[13] The structural parameters for the bridging acyl group are in support of the oxycarbene formulation as suggested by the ^{13}C NMR data (vide infra).

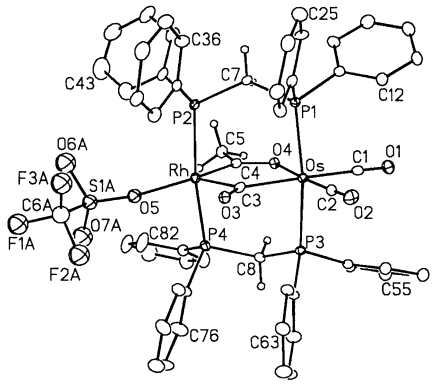

Figure 2. Perspective view of the complex cation of $[RhOs(CF_3SO_3)(CO)_2(\mu\text{-}CO)(\mu\text{-}C(CH_3)O)(dppm)_2][CF_3SO_3]$ (**3**) showing the atom-labeling scheme. Non-hydrogen atoms are represented by Gaussian ellipsoids at the 20% probability level. Hydrogen atoms are shown with arbitrarily small thermal parameters. The dppm phenyl hydrogens are not shown. Only the major occupant for the disordered coordinated triflate group is shown.

The long Rh−Os separation (3.4417(6) Å) is much longer than the intraligand P−P separations (3.168(2) and 3.161(2) Å) and is consistent with the absence of a metal−metal bond, resulting in a large Rh−C(3)−Os angle of 113.1(3)°. Although the Rh−C(3) and Os−C(3) distances (2.026(7), 2.098(7) Å) suggest a close-to-symmetric binding of the bridging carbonyl, the angles at C(3) (Os−C(3)−O(3) = 132.8(5)°, Rh−C(3)−O(3) = 114.0(5)°) indicate asymmetric binding of this carbonyl group. We suggest that this asymmetry may result from close interactions of this carbonyl with the ortho hydrogens of the dppm phenyl rings. Four short O(3)−H nonbonded contacts, of between 2.41 and 2.68 Å, involving phenyl rings 2, 3, 6, and 7, appear to be important in influencing the orientation of the bridging carbonyl group (C(3)O(3)), as shown in Figure 2.

The X-ray structure determination of **3** also reveals that one of the triflate anions is bound to Rh opposite the acyl group, with a normal Rh−O(5) distance of 2.237(6) Å. We assume that the solution structure matches that observed in the solid state, having the triflate ion coordinated to Rh. Not only is this necessary in order to achieve a 16-electron configuration, but the ^{13}C NMR spectral data in solution clearly show the carbonyl and acyl ligands in the arrangement shown in the solid state structure, leaving no other ligand except triflate to coordinate to a terminal site on Rh. However, the spectral data regarding triflate ion coordination are equivocal. The IR spectra of **3**, in the solid state and in solution, contain peaks in the 1200−1300 cm^{-1} region but no significant signals in the 1300−1400 cm^{-1} area, which are typically observed for covalently bound triflate groups.[31] The ^{19}F NMR spectrum has also been examined in order to determine the nature of the triflate

(30) (a) Erker, G. *Angew. Chem., Int. Ed. Engl.* **1989**, *28*, 397. (b) Schubert, U. *Coord. Chem. Rev.* **1984**, *55*, 261.

(31) Lawrance, G. A. *Chem. Rev.* **1986**, *86*, 17.

Table 3. Selected Interatomic Distances and Angles for Compound 3

(i) Distances (Å)

atom1	atom2	distance	atom1	atom2	distance
Os	Rh	3.4417(6)[a]	S(1B)	C(6B)	1.809(5)
Os	P(1)	2.392(2)	P(1)	P(2)	3.168(2)[a]
Os	P(3)	2.397(2)	P(1)	C(7)	1.851(7)
Os	O(4)	2.128(4)	P(2)	C(7)	1.829(7)
Os	C(1)	1.957(8)	P(3)	P(4)	3.161(2)[a]
Os	C(2)	1.873(7)	P(3)	C(8)	1.829(7)
Os	C(3)	2.098(7)	P(4)	C(8)	1.854(7)
Rh	P(2)	2.375(2)	F(1A)	C(6A)	1.32(2)[b]
Rh	P(4)	2.366(2)	F(2A)	C(6A)	1.41(2)[b]
Rh	O(5)	2.237(6)	F(3A)	C(6A)	1.28(2)[b]
Rh	C(3)	2.026(7)	F(1B)	C(6B)	1.35[c]
Rh	C(4)	1.907(7)	F(2B)	C(6B)	1.35[c]
S(1A)	O(5)	1.435(7)[b]	F(3B)	C(6B)	1.35[c]
S(1A)	O(6A)	1.51(2)[b]	O(1)	C(1)	1.126(9)
S(1A)	O(7A)	1.44(2)[b]	O(2)	C(2)	1.146(9)
S(1A)	C(6A)	1.76(2)[b]	O(3)	C(3)	1.175(8)
S(1B)	O(5)	1.45(1)[b]	O(4)	C(4)	1.258(8)
S(1B)	O(6B)	1.42(3)[b]	C(4)	C(5)	1.51(1)
S(1B)	O(7B)	1.42(3)[b]			

(ii) Angles (deg)

atom1	atom2	atom3	angle	atom1	atom2	atom3	angle
P(1)	Os	P(3)	171.42(6)	O(5)	S(1B)	C(6B)	93.3(8)
P(1)	Os	O(4)	85.5(2)	O(6B)	S(1B)	O(7B)	121(2)
P(1)	Os	C(1)	93.6(2)	O(6B)	S(1B)	C(6B)	99(2)
P(1)	Os	C(2)	93.2(2)	O(7B)	S(1B)	C(6B)	106(2)
P(1)	Os	C(3)	88.1(2)	Os	P(1)	C(7)	112.5(2)
P(3)	Os	O(4)	87.5(2)	Rh	P(2)	C(7)	112.1(2)
P(3)	Os	C(1)	91.0(2)	Os	P(3)	C(8)	111.7(3)
P(3)	Os	C(2)	94.1(2)	Rh	P(4)	C(8)	112.9(2)
P(3)	Os	C(3)	86.8(2)	Os	O(4)	C(4)	120.1(4)
O(4)	Os	C(1)	87.6(2)	Rh	O(5)	S(1A)	138.0(4)
O(4)	Os	C(2)	177.7(3)	Rh	O(5)	S(1B)	131.0(5)
O(4)	Os	C(3)	87.9(2)	Os	C(1)	O(1)	178.5(7)
C(1)	Os	C(2)	90.7(3)	Os	C(2)	O(2)	178.2(7)
C(1)	Os	C(3)	175.1(3)	Os	C(3)	Rh	113.1(3)
C(2)	Os	C(3)	93.9(3)	Os	C(3)	O(3)	132.8(5)
P(2)	Rh	P(4)	171.16(7)	Rh	C(3)	O(3)	114.0(5)
P(2)	Rh	O(5)	95.9(2)	Rh	C(4)	O(4)	125.3(5)
P(2)	Rh	C(3)	87.3(2)	Rh	C(4)	C(5)	118.8(5)
P(2)	Rh	C(4)	86.4(2)	O(4)	C(4)	C(5)	115.8(6)
P(4)	Rh	O(5)	92.9(2)	S(1A)	C(6A)	F(1A)	111(1)
P(4)	Rh	C(3)	92.0(2)	S(1A)	C(6A)	F(2A)	109(1)
P(4)	Rh	C(4)	84.9(2)	S(1A)	C(6A)	F(3A)	116(1)
O(5)	Rh	C(3)	99.3(2)	F(1A)	C(6A)	F(2A)	104(1)
O(5)	Rh	C(4)	167.1(2)	F(1A)	C(6A)	F(3A)	108(2)
C(3)	Rh	C(4)	93.5(3)	F(2A)	C(6A)	F(3A)	109(2)
O(5)	S(1A)	O(6A)	116.4(7)	S(1B)	C(6B)	F(1B)	113(2)
O(5)	S(1A)	O(7A)	115.3(7)	S(1B)	C(6B)	F(2B)	109(2)
O(5)	S(1A)	C(6A)	104.0(7)	S(1B)	C(6B)	F(3B)	105(2)
O(6A)	S(1A)	O(7A)	110.9(9)	F(1B)	C(6B)	F(2B)	117(2)
O(6A)	S(1A)	C(6A)	101.4(8)	F(1B)	C(6B)	F(3B)	92(2)
O(7A)	S(1A)	C(6A)	107.1(9)	F(2B)	C(6B)	F(3B)	120(2)
O(5)	S(1B)	O(6B)	119(1)	P(1)	C(7)	P(2)	118.8(4)
O(5)	S(1B)	O(7B)	112(1)	P(3)	C(8)	P(4)	118.2(4)

[a] Nonbonded distance. [b] Atoms labeled A correspond to the major occupant of the disordered triflate group, while B corresponds to the minor occupant. [c] Distance fixed during refinement.

group in solution. However there appears to be no perceptible difference in the ^{19}F chemical shifts between free and coordinated triflate in this case. Further confirmation of triflate ion coordination is obtained from the electrospray mass spectrum, which shows a parent peak at 1339 amu, which indicates a monocationic parent ion containing a coordinated triflate group.

Although the triflate anion is coordinated in CH_2Cl_2 and THF solutions of **3**, the bonding is relatively weak, and this anion can be readily displaced by more strongly coordinating ligands such as CO and PMe_3. Addition of CO to a solution of the tricarbonyl species [RhOs(CF_3SO_3)$(CO)_2$(μ-CO)(μ-C(CH_3)O)(dppm)$_2$][CF_3SO_3] (**3**) at −80 °C results in the formation of the tetracarbonyl species [RhOs$(CO)_3$(μ-CO)(μ-C(CH_3)O)(dppm)$_2$][CF_3SO_3]$_2$ (**4**) (Scheme 2). In the ^1H NMR spectrum the protons of the acetyl group appear as a singlet at δ 1.81, while the dppm-methylene protons are observed as multiplets at δ 3.44 and 3.86. The ^{13}C NMR spectrum of a ^{13}CO-enriched sample displays five signals: a doublet of multiplets at δ 321.8 ($^1J_{Rh-C}$ = 30 Hz) represents the rhodium-bound acyl carbon; a multiplet at δ 223.9 is consistent with a bridging carbonyl; a doublet of multiplets at δ 187.6 is due to the carbonyl group bound to

Scheme 2

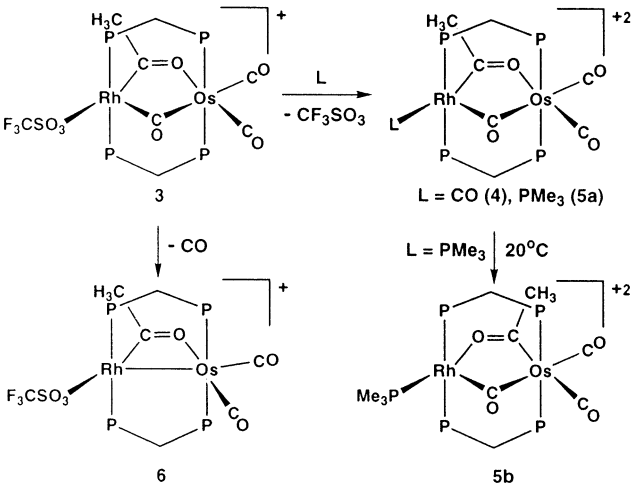

Scheme 3

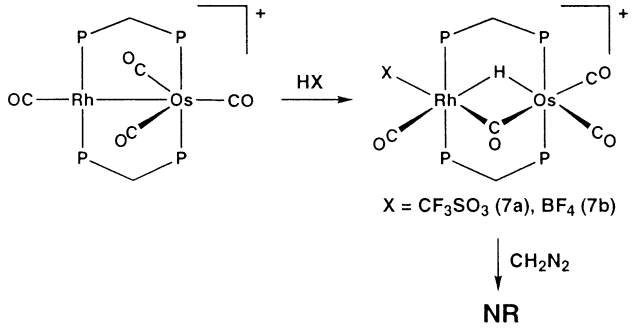

Rh ($^1J_{Rh-C}$ = 47 Hz), which we suggest has taken the coordination site previously occupied by the triflate anion; and two broad singlets at δ 171.4 and 172.3 are due to the osmium-bound carbonyls. The Rh-bound carbonyl, however, is relatively weakly coordinated and is readily replaced by the triflate group, re-forming compound **3**, at temperatures greater than −60 °C. It is interesting that the coupling to Rh of this labile carbonyl (47 Hz) is substantially less than normally observed for terminal carbonyls (ca. 60−80 Hz).

Addition of PMe_3 to **3** at −40 °C results in replacement of the coordinated triflate by PMe_3 (Scheme 2) to yield $[RhOs(PMe_3)(CO)_2(\mu\text{-}CO)(\mu\text{-}C(CH_3)O)(dppm)_2][CF_3SO_3]_2$ (**5a**). In the ^{31}P NMR spectrum the rhodium- and osmium-bound dppm-phosphorus nuclei appear as a doublet of multiplets at δ 14.5 ($^1J_{Rh-P}$ = 137 Hz) and a multiplet at δ −3.9, respectively, while the PMe_3 signal appears as a doublet of multiplets at δ −39.3 ($^1J_{Rh-P}$ = 101 Hz). The ^{13}C NMR spectrum of **5a** again shows the characteristic downfield signal for the acyl carbonyl (δ 325.8, $^1J_{Rh-C}$ = 30 Hz) with a large doublet coupling ($^2J_{P-C}$ = 82 Hz) to the PMe_3 group, suggesting that the phosphine is located trans to the acyl carbon in the site of the displaced triflate anion. This has been confirmed by an X-ray structure determination.[32] A multiplet at δ 237.0 is indicative of a bridging carbonyl, and two multiplets at δ 174.8 and 171.2 are due to the osmium-bound carbonyls.

Upon warming **5a** to ambient temperature, a new species (**5b**), having the same formulation as **5a**, appears. The only difference appears to be in the coordination mode of the acetyl group, which is reversed in **5b**, having the acyl carbon bound to Os. This acyl carbon appears as a narrow multiplet at δ 293.4 and displays no obvious coupling to Rh or to the PMe_3 group, which remains bound to Rh as shown by the coupling to this nucleus of 100 Hz. The bridging carbonyl in **5b** resonates at δ 218.1 in the ^{13}C NMR spectrum, and those of the Os-bound carbonyls appear at δ 183.0 and 172.5. The lower-field terminal carbonyl appears to be opposite the acyl carbonyl as shown by selective $^{13}C-^{13}C$ decoupling experiments of a ^{13}CO-labeled sample.

Replacement of the triflate anions by tetrafluoroborate, by protonation of $[RhOs(CO)_4(\mu\text{-}CH_2)(dppm)_2][BF_4]$ using HBF_4, yields both low-temperature compounds **1** and **2** as the BF_4^- salts. However, upon warming to room temperature, conversion to the BF_4^- salt of **3** is not observed; instead decomposition to a mixture of several products occurs. Thus, it appears that coordination of the triflate group is necessary to stabilize the acyl compound **3**, and apparently the poorer coordinating ability of BF_4^- [33] is insufficient to stabilize the acetyl-bridged species as the BF_4^- adduct. Since the low-temperature NMR spectra (^{31}P, ^{13}C, ^1H) of either **1** or **2**, having either triflate or tetrafluoroborate anions, are identical, it seems clear that these compounds do not have coordinated anions.

In the synthesis of **3** by the above route another species was observed as a minor (∼10%) impurity; this product can be quantitatively obtained upon refluxing **3** in CH_2Cl_2 for 1 h under an argon purge. The ^1H NMR spectrum of this new compound contains a singlet at δ 2.02 representative of an acyl methyl group, and the electrospray mass spectrum of this new compound is consistent with the dicarbonyl formulation, $[RhOs(CF_3SO_3)(CO)_2(\mu\text{-}C(CH_3)O)(dppm)_2][CF_3SO_3]$ **(6)**. This formulation is supported by the IR spectrum, which displays bands at 2033 and 1974 cm^{-1} for the terminal carbonyls; again no stretch is obvious for the acyl group. In addition, the $^{13}C\{^1H\}$ NMR spectrum of a ^{13}CO-enriched sample shows only three resonances at δ 274.2, 181.6, and 163.2, corresponding to the acyl and two terminal carbonyl groups, respectively. Although the high-field carbonyl resonance displays a 6 Hz coupling to rhodium, suggesting a possible weak interaction with this metal (possibly through a weak semibridging interaction), the chemical shift is inconsistent with any bridging interaction. We therefore propose that this carbonyl occupies the site on osmium opposite the Rh−Os bond. Two-bond $^{103}Rh-^{13}C$ coupling via the metal−metal bond has previously been observed with carbonyls in the site trans to the Rh−M bond.[34]

Again this structural formulation of **6** is confirmed by the X-ray structure determination, as shown in Figure 3. Relevant bond lengths and angles are summarized in Table 4. The most obvious structural differences between **3** and **6** are the absence of the bridging carbonyl in the latter and the substantial compression of the Rh−Os separation from 3.4417(6) Å in **3** to

(32) Ferguson, M. J.; Trepanier, S. J.; Cowie, M. Unpublished data. The data quality was sufficient for unambiguous location of all non-hydrogen atoms but was not of publication quality.

(33) Beck, W.; Sünkel, K. *Chem. Rev.* **1988**, *88*, 1405.

(34) (a) Jenkins, J. A.; Cowie, M. *Organometallics* **1992**, *11*, 2767. (b) Sterenberg, B. T., Ph.D. Thesis, University of Alberta, 1997, p 45.

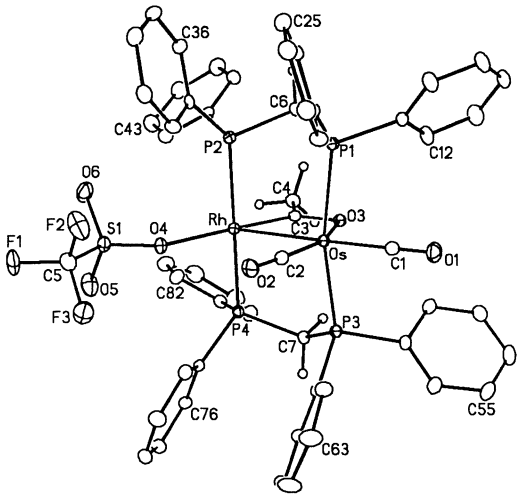

Figure 3. Perspective view of the complex cation of [RhOs(CF_3SO_3)$(CO)_2$(μ-C(CH_3)O)$(dppm)_2$][CF_3SO_3] (**6**) showing the atom-labeling scheme. Thermal ellipsoids are as for Figure 2.

2.7061(4) Å in **6**. This compression has little influence on the bond lengths within the bridging acetyl group. As a result, the Rh−acyl distance (Rh−C(3) = 1.913(5) Å) and the acyl carbonyl distance (C(3)−O(3) = 1.271(6) Å) again suggest involvement of the carbene structure **F**, shown earlier. In addition, compression along the metal−metal axis also has had little effect on the angles at the acyl carbon, with all remaining near the idealized value of 120°. The major change in the acyl binding shows up in the C(3)−O(3)−Os angle, which has been compressed from 120.1(4)° in **3** to 100.8(3)° in **6**.

The geometry at Os can be described as a distorted octahedral coordination, whereas that of Rh can be regarded as a tetragonal pyramid having the surrounding ligands in the square plane and Os in the fifth site. The diphosphine ligands have the typical trans arrangement at Rh (P(2)−Rh−P(4) = 167.76(5)°), while the acetyl carbon is trans (O(4)−Rh−C(3) = 178.8(2)°) to the oxygen atom of a coordinated triflate group. The triflate oxygen−Rh bond distance (Rh−O(4)) is 2.218(3) Å, similar to that in compound **3**. Again the ^{13}C NMR data and X-ray-derived structural data are in agreement and support an oxy-carbene character of the bridging acetyl group.

At osmium, the major distortion from idealized octahedral geometry results from the bridging nature of the acetyl group, which results in an acute Rh−Os−O(3) angle (69.06(9)°) and an obtuse C(1)−Os−O(3) angle (107.5(2)°). In addition, the P(1)−Os−P(3) angle (164.73(5)°) is substantially distorted from 180°, reflecting the attraction of both metals as a result of metal−metal bonding. The Rh−Os separation (2.7061(4) Å) is typical of a Rh−Os single bond.

We have also attempted to generate the cationic acetyl-bridged species (**3**) by reaction of the appropriate hydride species with diazomethane. These hydride complexes, [RhOsX$(CO)_3$(μ-H)(μ-CO)$(dppm)_2$][X] (X = CF_3SO_3 (**7a**), BF_4 (**7b**)), were obtained by protonation of the appropriate precursor [RhOs$(CO)_4(dppm)_2$][X] with the acid having the corresponding anion. For **7a** the hydride resonance appears as a doublet of multiplets at δ −10.5 in the ^1H NMR spectrum ($^1J_{Rh-H}$ = 21 Hz, $^2J_{P(Os)-H}$ = 8 Hz, $^2J_{P(Rh)-H}$ = 9 Hz). The comparable coupling of the hydride ligand to both sets of ^{31}P nuclei (Rh- and Os-bound) suggests that this hydride is symmetrically bridging. The $^{13}C\{^1H\}$ NMR spectrum at ambient temperature shows four carbonyl resonances; a doublet of triplets at δ 181.8 ($^1J_{Rh-C}$ = 79 Hz; $^2J_{P-H}$ = 15 Hz) is due to a Rh-bound carbonyl, a slightly broadened singlet at δ 169.4 is due to an Os-bound carbonyl, and two very broad signals at δ 200.0 and 171.8 are also due to Os-bound carbonyls. At −90 °C all signals sharpen somewhat, although coupling of the Os-bound carbonyls to the adjacent ^{31}P nuclei is never resolved. Nevertheless, the absence of Rh coupling in these signals establishes that they are on Os. The low-field signal suggests a weakly semibridging bonding mode for which Rh coupling is not resolved. A spin-saturation-transfer experiment, in which irradiation of the carbonyl signal at δ 171.8 leads to the disappearance of the signal at δ 200.0, indicates that the carbonyls giving rise to these signals ($(CO)_C$ and $(CO)_A$) are exchanging. This most probably occurs by tunneling of the hydride between the metals accompanied by rotation of the metal−carbonyl framework as shown in Chart 4 (dppm ligands above and below the plane of the drawing are omitted). Dissociation of the triflate anion and recoordination is also presumed to occur in this exchange mechanism. However, the addition of 5 equiv of sodium triflate to a solution of **7a** resulted in no noticeable change in any of the NMR spectra between ambient temperature and −80 °C, so the influence of triflate dissociation on this exchange process could not be established.

Chart 4

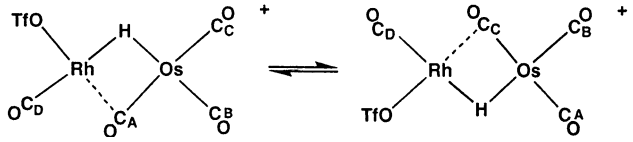

The BF_4^- analogue of **7a**, namely, [RhOs$(FBF_3)(CO)_3$(μ-H)(μ-CO)$(dppm)_2$][BF_4] (**7b**), was prepared using HBF_4. This species has spectral parameters almost identical to that of **7a**. At ambient temperature only one broad signal, at δ −151.3, was observed in the ^{19}F NMR spectrum for the BF_4^- anions. However, at −90 °C two signals are observed at δ −153.9, corresponding to free BF_4^-, and at −149.7 for the coordinated BF_4^-; the latter signal appears somewhat broader than the other. Both signals appear as two peaks in an approximate 1:4 ratio, corresponding to the relative abundance of ^{10}B and ^{11}B isotopes. We propose that **7b** has the BF_4^- anion coordinated to Rh, analogous to the triflate anion in **7a**. The absence of Rh coupling to the coordinated BF_4^- group presumably results from a combination of weak BF_4^- coordination and exchange of all four fluorines on this group between Rh-bound and unbound sites. This proposal has been supported by a poor quality X-ray structure determination of **7b**, which showed a disordered BF_4^- group bound to Rh.[32] We had previously reported **7b**,[16] but at the time had failed to recognize that one BF_4^- anion was coordinated.

In any case, the spectral similarities of **7a** and **7b** suggest comparable structures and the structure of **7a** has been unambiguously established by X-ray crystallography, as shown in Figure 4, which clearly shows

Table 4. Selected Interatomic Distances and Angles for Compound 6

(i) Distances (Å)

atom1	atom2	distance	atom1	atom2	distance
Os	Rh	2.7061(4)	P(1)	P(2)	2.978(2)[a]
Os	P(1)	2.410(1)	P(1)	C(6)	1.826(5)
Os	P(3)	2.415(1)	P(2)	C(6)	1.825(5)
Os	O(3)	2.150(3)	P(3)	P(4)	2.979(2)[a]
Os	C(1)	1.883(5)	P(3)	C(7)	1.825(5)
Os	C(2)	1.882(5)	P(4)	C(7)	1.832(5)
Rh	P(2)	2.329(1)	F(1)	C(5)	1.321(7)
Rh	P(4)	2.325(1)	F(2)	C(5)	1.313(7)
Rh	O(4)	2.218(3)	F(3)	C(5)	1.321(7)
Rh	C(3)	1.913(5)	O(1)	C(1)	1.138(6)
S(1)	O(4)	1.456(4)	O(2)	C(2)	1.138(6)
S(1)	O(5)	1.410(5)	O(3)	C(3)	1.271(6)
S(1)	O(6)	1.431(5)	C(3)	C(4)	1.516(6)
S(1)	C(5)	1.824(6)			

(ii) Angles (deg)

atom1	atom2	atom3	angle	atom1	atom2	atom3	angle
Rh	Os	P(1)	92.82(4)	O(4)	S(1)	O(5)	113.8(3)
Rh	Os	P(3)	93.01(3)	O(4)	S(1)	O(6)	113.6(3)
Rh	Os	O(3)	69.06(9)	O(4)	S(1)	C(5)	101.9(2)
Rh	Os	C(1)	176.5(2)	O(5)	S(1)	O(6)	116.7(3)
Rh	Os	C(2)	90.1(2)	O(5)	S(1)	C(5)	104.3(3)
P(1)	Os	P(3)	164.73(5)	O(6)	S(1)	C(5)	104.4(3)
P(1)	Os	O(3)	84.1(1)	Os	P(1)	C(6)	110.2(2)
P(1)	Os	C(1)	86.5(2)	Rh	P(2)	C(6)	110.7(2)
P(1)	Os	C(2)	97.2(2)	Os	P(3)	C(7)	110.2(2)
P(3)	Os	O(3)	84.8(1)	Rh	P(4)	C(7)	112.5(2)
P(3)	Os	C(1)	86.8(2)	Os	O(3)	C(3)	100.8(3)
P(3)	Os	C(2)	96.9(2)	Rh	O(4)	S(1)	133.8(2)
O(3)	Os	C(1)	107.5(2)	Os	C(1)	O(1)	177.1(5)
O(3)	Os	C(2)	159.1(2)	Os	C(2)	O(2)	173.9(4)
C(1)	Os	C(2)	93.4(2)	Rh	C(3)	O(3)	121.1(3)
Os	Rh	P(2)	93.64(4)	Rh	C(3)	C(4)	123.9(3)
Os	Rh	P(4)	93.57(4)	O(3)	C(3)	C(4)	115.0(4)
Os	Rh	O(4)	110.19(9)	S(1)	C(5)	F(1)	110.8(4)
Os	Rh	C(3)	69.0 (1)	S(1)	C(5)	F(2)	112.1(4)
P(2)	Rh	P(4)	167.76(5)	S(1)	C(5)	F(3)	110.2(4)
P(2)	Rh	O(4)	94.0(1)	F(1)	C(5)	F(2)	107.4(5)
P(2)	Rh	C(3)	87.0(2)	F(1)	C(5)	F(3)	107.6(5)
P(4)	Rh	O(4)	92.8(1)	F(2)	C(5)	F(3)	108.5(5)
P(4)	Rh	C(3)	86.4(2)	P(1)	C(6)	P(2)	109.3(3)
O(4)	Rh	C(3)	178.8(2)	P(3)	C(7)	P(4)	109.1(3)

[a] Nonbonded distance.

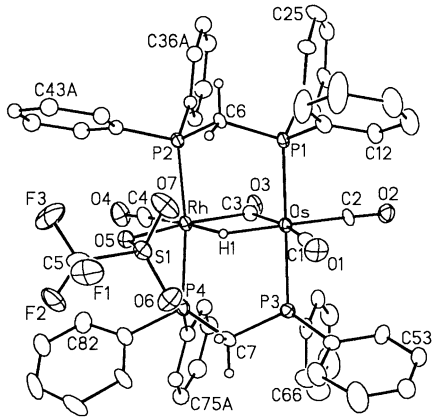

Figure 4. Perspective view of the complex cation of [RhOs-

that the triflate anion is coordinated to Rh opposite the bridging carbonyl. Both metals have distorted octahedral geometries in which the octahedra share an edge at the bridging hydride and carbonyl groups. Much of the distortion at both metals results from the smaller steric demands of the hydride ligand, leading to an opening up of the angles between the other ligands in the plane containing the metals and the bridging hydride; these angles range from 96.2(5)° to 102.5(5)°, as given in Table 5. Carbonyl C(1)O(1), opposite the bridging carbonyl, has the longest metal−carbonyl distance, and the Rh−O(5) distance (2.424(7) Å), involving the coordinated triflate ion, also opposite the bridging carbonyl, is also significantly longer than the analogous distances in compounds **3** and **6** (2.237(6) and 2.218(3) Å, respectively).

Attempts to generate compound **3** by reaction of **7a** with diazomethane failed; no reaction occurred even after extended reaction times in the presence of excess CH_2N_2. Similarly the BF_4^- salt (**7b**) also failed to react with diazomethane.

Discussion

Protonation of the methylene-bridged compound [RhOs(CO)$_4$(μ-CH$_2$)(dppm)$_2$][CF$_3$SO$_3$] with CF$_3$SO$_3$H at −80 °C results in the formation of an osmium-bound methyl complex (**1**) in which the methyl group is asymmetrically bridging and involved in an agostic interaction with rhodium. The donation of the pair of C−H electrons of the agostic bridging methyl group to Rh is presumably necessary to alleviate the electron deficiency brought

Table 5. Selected Interatomic Distances and Angles for Compound 7a

(i) Distances (Å)

atom1	atom2	distance	atom1	atom2	distance
Os	Rh	2.8742(9)	S(1)	O(7)	1.44(1)
Os	P(1)	2.383(3)	S(1)	C(5)	1.85(1)
Os	P(3)	2.382(3)	P(1)	P(2)	3.018(4)[b]
Os	C(1)	1.96(1)	P(1)	C(6)	1.82(1)
Os	C(2)	1.879(9)	P(2)	C(6)	1.85(1)
Os	C(3)	2.05(1)	P(3)	P(4)	3.005(4)[b]
Os	H(1)	1.85[a]	P(3)	C(7)	1.84(1)
Rh	P(2)	2.360(3)	P(4)	C(7)	1.79(1)
Rh	P(4)	2.371(3)	F(1)	C(5)	1.35(2)
Rh	O(5)	2.424(7)	F(2)	C(5)	1.31(2)
Rh	C(3)	2.08(1)	F(3)	C(5)	1.32(2)
Rh	C(4)	1.84(1)	O(1)	C(1)	1.13(2)
Rh	H(1)	1.85[a]	O(2)	C(2)	1.17(1)
S(1)	O(5)	1.451(8)	O(3)	C(3)	1.20(1)
S(1)	O(6)	1.44(1)	O(4)	C(4)	1.16(1)

(ii) Angles (deg)

atom1	atom2	atom3	angle	atom1	atom2	atom3	angle
Rh	Os	P(1)	91.49(7)	O(5)	Rh	C(4)	99.1(4)
Rh	Os	P(3)	89.80(8)	C(3)	Rh	C(4)	102.5(5)
Rh	Os	C(1)	119.9(4)	O(5)	S(1)	O(6)	113.9(5)
Rh	Os	C(2)	144.0(3)	O(5)	S(1)	O(7)	114.3(5)
Rh	Os	C(3)	46.4(3)	O(5)	S(1)	C(5)	102.3(7)
P(1)	Os	P(3)	174.0(1)	O(6)	S(1)	O(7)	116.6(7)
P(1)	Os	C(1)	86.7(4)	O(6)	S(1)	C(5)	104.5(6)
P(1)	Os	C(2)	90.6(3)	O(7)	S(1)	C(5)	102.8(7)
P(1)	Os	C(3)	93.4(3)	Os	P(1)	C(6)	111.0(4)
P(3)	Os	C(1)	87.6(4)	Rh	P(2)	C(6)	110.2(4)
P(3)	Os	C(2)	91.8(3)	Os	P(3)	C(7)	110.5(4)
P(3)	Os	C(3)	91.7(3)	Rh	P(4)	C(7)	110.2(4)
C(1)	Os	C(2)	96.2(5)	Rh	O(5)	S(1)	119.8(4)
C(1)	Os	C(3)	166.2(5)	Os	C(1)	O(1)	177(1)
C(2)	Os	C(3)	97.6(4)	Os	C(2)	O(2)	179(1)
Os	Rh	P(2)	91.96(8)	Os	C(3)	Rh	88.3(4)
Os	Rh	P(4)	93.27(8)	Os	C(3)	O(3)	145.0(9)
Os	Rh	O(5)	113.0(2)	Rh	C(3)	O(3)	126.8(9)
Os	Rh	C(3)	45.4(3)	Rh	C(4)	O(4)	179(1)
Os	Rh	C(4)	147.9(4)	S(1)	C(5)	F(1)	109(1)
P(2)	Rh	P(4)	170.6(1)	S(1)	C(5)	F(2)	109(1)
P(2)	Rh	O(5)	86.8(2)	S(1)	C(5)	F(3)	109.7(9)
P(2)	Rh	C(3)	92.5(3)	F(1)	C(5)	F(2)	111(1)
P(2)	Rh	C(4)	90.8(4)	F(1)	C(5)	F(3)	107(1)
P(4)	Rh	O(5)	84.0(2)	F(2)	C(5)	F(3)	111(2)
P(4)	Rh	C(3)	96.7(3)	P(1)	C(6)	P(2)	110.6(6)
P(4)	Rh	C(4)	88.9(4)	P(3)	C(7)	P(4)	112.0(6)
O(5)	Rh	C(3)	158.4(3)	Os	H(1)	Rh	101.9

[a] Distance fixed during refinement. [b] Nonbonded distance.

about by the dicationic charge of the complex. This agostic interaction appears to facilitate the migration of the methyl group from one metal to the other by bringing this osmium-bound methyl group into a simultaneous bonding interaction with rhodium. From this bridging position in **1** methyl transfer to Rh occurs at −40 °C to give **2**. Why this migration occurs is not clear, although we assume that the stabilization gained from the stronger Os−CO versus Rh−CO bond[35] is greater than that lost by conversion of a stronger Os−CH_3 bond to a weaker Rh−CH_3 bond.[35] It should also be pointed out, however, that the exchange of an agostic interaction in **1** for a semibridging carbonyl in **2** may also favor the observed transformation.

Warming a solution of **2** to ambient temperature results in migratory insertion of the methyl and a carbonyl group, yielding a bridging acetyl complex. The formation of the acetyl group from **2** rather than **1** can be understood on the basis of the migratory insertion tendencies of a second-row versus a third-row metal.[11] It seems likely that migratory insertion is favored when the methyl group is on Rh, due to the weaker Rh−CH_3 bond compared to the Os−CH_3 bond. In addition, methyl migratory insertion in **2** appears to be facilitated by the semibridging carbonyls which are positioned suitably for migratory insertion of a rhodium-bound methyl group.

Coordination of a triflate anion to rhodium appears to be necessary to stabilize this acetyl-bridged complex, allowing Rh to have a 16-electron configuration. In contrast, the BF_4^- analogue (**2**-BF_4) does not transform to an acyl complex upon warming to 25 °C and instead decomposes to a mixture of products. The weaker coordinating ability of BF_4^- relative to $CF_3SO_3^-$ appears

(35) (a) Ziegler, T.; Tschinke, V. In *Bonding Energetics in Organometallic Compounds*; Marks, T. J., Ed.; American Chemical Society: Washington, DC, 1990; Chapter 19. (b) Ziegler, T.; Tschinke, V.; Urenbach, B. *J. Am. Chem. Soc.* **1987**, *1−0*, 4825. (c) Armentrout, P. B. In *Bonding Energetics in Organometallic Compounds*; Marks, T. J., Ed.; American Chemical Society: Washington, DC, 1990; Chapter 2.

to prevent formation of a stable BF_4^--coordinated acyl complex analogous to **3**. The coordination of $CF_3SO_3^-$, which is generally considered a weak donor group, is facilitated by the high electrophilicity of what would be a dicationic species without coordination of this anion. A similar example was observed by Puddephatt,[14] who recently reported that protonation of the complex $[Ru_2(CO)_4(\mu\text{-}CH_2)(dppm)_2]$ with various acids (HBF_4, CF_3SO_3H, HCO_2H, CH_3CO_2H) resulted in the formation of the cationic methyl complex $[Ru_2(CO)_4(\mu\text{-}CH_3)(dppm)_2]^+$, which was stable at low temperature. However, in this system only the formate and acetate complexes resulted in the formation of stable acetyl compounds at higher temperature; the BF_4^- and $CF_3SO_3^-$ anions had insufficient coordinating abilities to stabilize the acetyl species, resulting in decay of these compounds into a mixture of products.

The lability of the coordinated triflate anion in **3** is demonstrated by its facile displacement by CO and PMe_3. In both cases the initial products **4** and **5a**, observed at low temperature, appear to result from replacement of the triflate anion and substrate coordination at Rh. In the case of the PMe_3 adduct **5a**, an interesting transformation of the acetyl group occurs upon warming in which it reverses its coordination mode, becoming C-bound to Os rather than to Rh. This transformation may be initiated by the high trans effect of PMe_3, which labilizes the Rh−C(O)CH_3 linkage in the initial adduct **5a**. We were unable to detect any intermediates in the transformation of **5a** to **5b** and are unable to speculate on how this rearrangement occurs. To our knowledge this reversal in coordination of a bridging acetyl group is unprecedented.

One of the carbonyls in $[RhOs(CF_3SO_3)(CO)_2(\mu\text{-}CO)(\mu\text{-}C(CH_3)O)(dppm)_2][CF_3SO_3]$ (**3**) is labile and is lost slowly at ambient temperature or rapidly in refluxing CH_2Cl_2 to give the dicarbonyl complex **6**. Loss of a carbonyl is accompanied by the formation of a metal−metal bond in order to maintain 16- and 18-electron configurations of Rh and Os, respectively. The nature of this metal−metal interaction is clearly dependent on the bonding formulation for the acetyl group. If an oxycarbene formulation is considered, the oxidation states are best thought of as Rh^{1+}/Os^{2+}, in which the square-planar Rh^{1+} center forms a dative bond via its d_{z^2} orbital to Os^{2+}, giving the latter the expected 18-electron configuration. We favor this description over an acetyl formulation, which would yield the Rh^{3+}/Os^0 combination of oxidation states, in which the Rh^{3+} center achieves a 16-electron configuration via an Os→Rh dative bond. Although structures **3**−**6** are all drawn in the Schemes with bridging acetyl formulations, we consider their bonding more consistent with oxycarbenes. Surprisingly perhaps, carbonyl loss from **3** is not accompanied by "deinsertion" of the acyl carbonyl to give methyl and carbonyl groups. This may be a consequence of the carbene-like bonding of this group, or may simply be related to its bridging coordination mode; bridging acyls are three-electron donors, so nothing is gained in terms of electron count by converting to a methyl and a carbonyl ligand.

We find it surprising that the hydride-bridged species **7a** and **7b** do not react with diazomethane; in the case of **7a** we had anticipated obtaining the acetyl-bridged **3**. Although we have observed failures of neutral bimetallic complexes such as $[RhIr(CO)_3(dppm)_2]$ and $[Ir_2(CO)_3(dppm)_2]$ to react with diazomethane,[36] cationic complexes such as $[MM'(CO)_4(dppm)_2]^+$ (M = Rh, Ir; M′ = Fe, Ru, Os) have reacted readily, giving the methylene-bridged species $[MM'(CO)_3(\mu\text{-}CH_2)(\mu\text{-}CO)(dppm)_2]^+$.[2−4,37] We assume that the failure of the cationic species **7a** and **7b** to react with diazomethane results from the coordinative saturation brought about by anion coordination in each case. Even these weakly associated anions appear to compete more effectively for a coordination site on Rh than diazomethane.

Relevance to FT Chemistry. A rationale for studying acetyl complexes was the possibility of converting these groups into oxygen-containing substrates via reaction with H_2. Such a transformation would mimic another step in the FT production of oxygenates. In this regard, the formulation of the bridging acetyl groups as oxycarbenes has potential implications for the involvement of such groups in ethanol formation. Whereas reaction of an η^1-acetyl group with H_2 is expected to yield acetaldehyde, a bridging oxycarbene may react differently. If initial hydrogen transfer to the carbene carbon occurred, a bridged α-oxyethyl group would result, and subsequent hydrogen transfer to oxygen followed by hydrogenolysis could yield ethanol. Alternately, if initial hydrogen transfer to the oxygen of the bridging acetyl group occurred, a hydroxycarbene would result, and hydrogenation of the metal−carbene linkage would give an α-hydroxy ethyl group, followed by reductive elimination of ethanol. Particularly relevant to the possibility of ethanol formation is the isomerization of **5a** to **5b** (Scheme 2), in which the acetyl group rearranges from one that is carbon-bound to Rh to one that is carbon-bound to Os and having a Rh−O bond. We assume that oxidative addition of H_2 will occur at the unsaturated Rh center. This being the case we might anticipate that the reaction of **5a** with H_2 would proceed by hydrogen atom transfer to the acetyl carbon. Although this could give rise to ethanol in the sequence described above, it could also result in acetaldehyde formation. However, in the "reverse acetyl" complex **5b**, oxidative addition at Rh could lead to initial hydrogen transfer to oxygen to give a hydroxycarbene, followed by subsequent hydrogen transfers to yield ethanol.

Unfortunately, the reactions of these acetyl-bridged complexes with hydrogen give no detectable amounts of ethanol. Whereas, compound **3** was found to be unreactive to H_2, reaction of **6** with H_2 did occur slowly at ambient temperature, but yielded a complex mixture of unidentified products. ^1H NMR spectra of the product mixture did establish the presence of a number of hydride species (as indicated by the high-field ^1H signals), but no oxygenates such as acetaldehyde or ethanol were detected. Compound **5a** did react readily with H_2; however the first product obtained was not an expected product of H_2 addition, but was merely the isomerization product **5b**. This isomerization occurs much more readily in the presence of H_2 than without, although what function H_2 has in this isomerization is not known. Under prolonged exposure to H_2, compound **5b** yields the known hydride species $[RhOs(CO)_3(\mu\text{-}H)_2$-

(36) Oke, O.; Torkelson, J. R.; Cowie, M. Unpublished results.
(37) Lo, J., Cowie, M. Unpublished results.

$(dppm)_2][CF_3SO_3]$.[16] Again, no evidence of either ethanol or acetaldehyde was observed by either ^1H NMR or mass spectral analyses. The only hydrocarbon detected was methane. Oxidative addition of H_2 to an acetyl-bridged species apparently does not occur. Instead, reverse migration of the methyl group from the acetyl carbonyl to a metal occurs, and it is the resulting methyl species that adds H_2, leading to reductive elimination of methane. The other products in this reaction were observed to be protonated trimethyl phosphine ($HPMe_3^+$) and free carbon monoxide.

Conclusions

Protonation of the bridging methylene group in $[RhOs(CO)_4(\mu\text{-}CH_2)(dppm)_2][CF_3SO_3]$ leads, through a number of interesting transformations, to the acetyl-bridged species $[RhOs(CF_3SO_3)(CO)_2(\mu\text{-}CO)(\mu\text{-}C(CH_3)O)(dppm)_2][CF_3SO_3]$, from which a series of related acetyl-bridged products can be generated. X-ray crystallography and ^{13}C NMR spectroscopy support an oxycarbene formulation for these acetyl groups, the potential relevance of which for the formation of ethanol has been pursued. We thought that the unprecedented isomerization of $[RhOs(CO)_3(PMe_3)(\mu\text{-}C(CH_3)O)(dppm)_2][CF_3SO_3]_2$ (**5a**), in which the acetyl group is C-bound to Rh and O-bound to Os, to **5b**, in which the acetyl oxygen is now bound to Rh while the carbonyl carbon is bound to Os, may have interesting ramifications relating to the formation of oxygenate products in the reaction of such species with H_2. Unfortunately, the goal of generating ethanol from any of these acetyl-bridged products has not been realized; methane is the only hydrocarbon detected. Nevertheless, the roles of the different metals in several of the important transformations leading to these acetyl-bridged species have been determined, and work is ongoing with different metal combinations[38] in attempts to obtain information about the possible role of bridging acetyl groups in oxygenate formation.

Acknowledgment. We thank the Natural Sciences and Engineering Research Council of Canada (NSERC) and the University of Alberta for financial support of this research and NSERC for funding the Bruker PLATFORM/SMART 1000 CCD diffractometer. MC thanks the University and the Killam Trusts for a Killam Annual Research Professorship.

Supporting Information Available: Tables of X-ray experimental details, atomic coordinates, interatomic distances and angles, anisotropic thermal parameters, and hydrogen parameters for compounds **3**, **6**, and **7a**. This material is available free of charge via the Internet at http://pubs.acs.org.

OM030282M

(38) Trepanier, S. J.; Xu, L.; Cowie, M. Unpublished results.